Journal of Applied Polymer Science

Effect of the Carbon Black Structure on the Stability and Efficiency of the Conductive Network in Polyethylene Composites

Danqi Ren, Shaodi Zheng, Shilin Huang, Zhengying Liu, Mingbo Yang
College of Polymer Science and Engineering, State Key Laboratory of Polymer Materials Engineering, Sichuan University, Chengdu 610065, Sichuan, People's Republic of China
Correspondence to: Z. Liu (E-mail: liuzhying@scu.edu.com)

ABSTRACT: Composites of high-density polyethylene (HDPE) with different kinds of carbon black (CB) were prepared through melt blending. The influence of the CB structure on the stability and efficiency of the conductive network in HDPE/CB composites were mainly investigated. Scanning electron microscopy was used to observe the morphology of the CB primary aggregates. The relationship between the temperature-resistivity behaviors of the composites and the crystallization behaviors of the matrix were also investigated. High-structure CB built an effective conductive network at a low filler content compared to the low-structure one because of its branched morphology. Therefore, the composite containing high-structure CB revealed a lower percolation threshold. The composite containing low-structure CB obtained a stronger positive temperature coefficient (PTC) intensity because the cluster network was fragile and easily damaged during matrix melting. The reproducibility of the results of PTC effect of the composite containing high-structure CB was better than that of the composite containing a low-structure one. © 2013 Wiley Periodicals, Inc. J. Appl. Polym. Sci. 129: 3382–3389, 2013

KEYWORDS: functionalization of polymers; microscopy; morphology; nanoparticles; nanowires and nanocrystals; polyolefins

Received 4 August 2012; accepted 17 September 2012; published online 27 February 2013
DOI: 10.1002/app.38606

INTRODUCTION

Most polymers are insulating materials. When electrically conductive fillers, such as carbon black (CB),[1–6] carbon fibers[7–10] or carbon annotates,[11–17] or graphite,[18] are compounded into polymers above a threshold concentration, a continuous filler network can be built up and a conductive polymer composite can be obtained.

The positive temperature coefficient (PTC) effect is the sharp increase in resistivity when the temperature is close to the melting temperature (T_m) of the polymer matrix. The resistivity of conductive polymer composites (CPCs) has a maximum peak, and then, it decreases drastically with further increases in temperature; this is the negative temperature coefficient (NTC) effect. PTC and NTC effects are related to the temperature dependence of the electrical resistivity of the composites. Up to this point, PTC materials have been extensively studied because they could be widely used in overcurrent protectors, self-regulating heaters, and shielding materials.[1,6,8,19] If one supposes that the percolation phenomenon is associated with the formation of a conductive network in CPCs, the PTC and NTC effects are reflections of the conductive network destruction and rebuilding during thermal processes. Recently, more and more researchers have paid attention to the temperature-resistivity behavior during cooling because the process can affect the room-temperature resistivity and the conductive reproducibility of the CPCs.[1,10–16] According to Dai et al.,[1] the resistivity of *in situ* CB-filled microfibrillar poly(ethylene terephthalate) (PET)/polyethylene (PE) composites increased abnormally during cooling below 100°C. Thermal residual stresses developed in the interface between the PET microfibrils and the PE matrix were responsible for the cooling-induced resistivity increase. Deng et al.[12] and Alig et al.[14] also observed an increase in the resistivity during crystallization in the copolymerization of polypropylene (PP) matrix filled with CB or multiwalled carbon nanotubes; this could have resulted from the reduction of the amorphous phase at the expense of the crystalline phase. However, a contrary phenomenon was reported by Lim et al.[15] and Li et al.,[16] who observed a higher electrical conductivity during cooling in ethylene-*co*-vinyl acetate (EVA)/multiwalled carbon nanotube nanocomposites and CNT/polycarbonate/PE nanocomposite. The increase in the density of the conductive network associated with the volume shrinkage of the polymer matrix when a sample crystallizes was used to explain the phenomenon.

CB is one of the most widely used conductive fillers for polymer-based composites. The primary properties of the CB particles influencing the properties of composites include their structure,

Table I. Types and Properties of the CB Used in the Experiment

Structure	Commercial name	DBP volume (mL/100 g)	Mean particle size (nm)	Specific surface area (m^2/g)	True bulk density (g/cm^3)[a]	Apparent bulk density (g/cm^3)[a]	ϕ_m
High	BP2000	330	15	1475	1.90	0.146	0.144
Medium	VXC-72	178	30	254	1.92	0.259	0.238
Low	VXC-68	123	25	68	—	—	0.311

[a]From ref. 20.

particle size, surface area, surface chemistry, and physical properties; among these, the structure of CB is the most important characteristic when the stability and the efficiency of the conductive network are considered. CB primary aggregates are composed of prime particles. The size and shape of the aggregates and the number of prime particles per aggregate determine the structure of CB. Because high-structure CB tends to produce larger aggregates in contact and aggregates separated by smaller distances, this results in a higher conductivity at the same loading[2,20] of particles. Mallette et al.[21] studied the rheological and electric properties of blends of PET and high-density polyethylene (HDPE) filled with various types of CB. They found that higher viscosities of the polymer melts during mixing were recorded in the composites containing high-structured CB; this indicated higher particle–polymer interactions. High conductivities were reached when HDPE containing the high-structure CB phase was dispersed in the PET matrix. Probst and Grivei[22] considered the structure and electrical properties of CB. The evolution of the volume of a given CB weight under increasing pressure and the evolution of the electrical resistivity were recorded and analyzed. They summarized that high-structure CB achieved a low resistivity at a very low particle density. In addition, when the CB particles were filled into polymer (PP or PE) at very low loading, the resistivity of the CB at a given volume fraction was at the same level in the compressed CB as in the polyolefins composite. Rahaman et al.[23] investigated the effect of the CB structure on the electromagnetic interference shielding effectiveness of EVA, nitrile-butadiene rubber (NBR), and their blends. They found that the samples filled with high-structure CB exhibited a higher conductivity and higher electromagnetic interference shielding effectiveness compared to those filled with the lower structure one at the same loading. Fathi et al.[24] researched the relationship between the CB structure and the low-strain conductivity of PP or low-density polyethylene (LDPE) composites. They suggested that the percolation threshold and optimum CB concentration were lower when the higher CB structure was used. What is more, the CB concentration for maximum strain sensitivity of the electrical conductivity was higher for low-structure CB, but it was essentially independent of the CB structure for the medium-structure to high-structure CBs.

However, as far as we know, all of the research works in this field have focused on the effect of the CB structure on the electrical conductivity performance at room temperature. For example, Fathi et al.[24] studied the influence of the CB structure on the low-strain conductivity of PP or LDPE composites at room temperature. What is more, they paid more attention to the phenomenon and ignored further explanation. Actually, a detailed investigation of the influence of the CB structure on the temperature-resistivity behavior of CPCs, let alone the resistivity differences during cooling, have yet to be published. As mentioned, the temperature dependence of the electrical resistivity has close ties to the stability and the efficiency of the conductive network in composites. In this study, the effect of the CB structure on the temperature-resistivity behavior of CPCs, including PTC, NTC effects, and the electrical reproducibility, were examined. More attention was centered on the resistivity variation during the cooling process. Our main purpose was to make use of the differences in the temperature-resistivity behavior to reveal the impacts of the CB structure on the stability and efficiency of the conductive network in CPCs.

EXPERIMENTAL

Materials and Sample Preparation

A commercial HDPE (2911, with a melt flow rate of 20 g/10 min at 190°C/2.16 kg, ASTM D 1238, supplied by Lanzhou Petroleum Chemical Co, Ltd., Lanzhou, China) was used as the matrix. The types and properties of the CB fillers used in this study are given in Table I. CB used in this article was supplied by Cabot Corp (Boston, Massachusetts, America). The HDPE/CB composites were prepared by melt mixing in a Haake mixer (XSS-300, Shanghai, China) at a temperature of 190°C and at 60 rpm for 10 min. The blends obtained were compressed into a plate with a thickness of 2 mm. Hot pressing was completed under a pressure of 10 MPa at 190°C for 5 min. Then, the tested samples were slowly cooled to room temperature under the same pressure. Before we performed the electrical measurements, all of the composites sheets were cut into testing samples ($10 \times 30 \times 2$ mm^3) and were rested overnight to release stress.

Characterization of the CB Particle Morphology

Scanning electron microscopy (SEM) observation was carried out with an Philips FEI INSPECT F instrument (Amsterdam, Holland). CB pellets were dispersed in alcohol by ultrasonic treatment, and some CB particles were collected on carbon-coated grids for SEM observation.

Electrical Properties of the HDPE/CB Composites

A two-probe method was used to perform room-temperature volume resistivity testing of the samples with a Keithley electrometer (6517B, Cleveland, Ohio, America)) when their resistivity was lower than 10^8 Ω cm. At both ends of the sample, the surface (10×2 mm^2) in contact with the copper electrodes was silver painted to ensure good contact, and a high-resistivity meter (ZC360, Shanghai, China) was used for samples with a higher resistivity (beyond 10^8 Ω.cm).

Applied Polymer SCIENCE

The volume resistivity of the conductive composites was measured as a function of temperature with a Huber thermostatic oil bath (Ministat230, Offenburg, Germany) to control the temperature and the Keithley 6517B electrometer to monitor the resistivity. The temperature varied from 25 to 190°C at a heating rate of 5°C/min and a cooling rate of 2°C/min. To keep good contact between the samples and the electrodes during the heating and cooling cycles, the copper electrodes were embedded into both ends of the sample (we heated the end of the sample and quickly squeezed the copper electrodes into the molten materials). Four heating and cooling cycles were carried out to check the reproducibility of the electrical conductivity results. In the first to third runs, the heating rate was 5°C/min and the cooling rate was 2°C/min. In the fourth run, heating rate was also 5°C/min, but the cooling rate was 1°C/min.

Differential Scanning Calorimetry (DSC)

Thermal analysis measurements were performed with a TA Q20 DSC instrument (Cranston, Rhode Island, America). A sample of about 5 mg of underwent the same thermal processing as the thermostatic oil bath. The temperature ranged from 25 to 190°C. In the first to third runs, the heating rate was 5°C/min, and the cooling rate was 2°C/min. In the fourth run, the heating rate was also 5°C/min, but the cooling rate was 1°C/min.

RESULTS AND DISCUSSION

CB Structure Observation

The most common method to describe CB structure is based on the measurement of the amount of dibutyl phthalate (DBP; an oil) absorbed by 100 g of CB. The CB with a greater amount of DBP absorption indicated a high-structure CB. The DBP absorption of CB used in this study is listed in Table I. BP2000 was a typical high-structure CB[21,25] with a DBP volume of 330 mL/100 g, and VXC-72 was a comparatively medium-structure CB[21,26] with a DBP volume of 178 mL/100 g. Meanwhile, the DBP absorption of VXC-68 was lowest of all of the used CBs (DBP volume = 123 mL/100 g) in this study. Mallette J G et al.[21] considered that the CB structural parameter is a measure of the three-dimensional distribution of CB particles in the form of clusters. The cluster distribution determines the apparent bulk density of CB. This density of CB is the relationship between the actual mass of carbon particles and the apparent volume occupied by the clusters. A high apparent density corresponds to a lower structure, and the highly structured CB normally possesses a low apparent density. The true bulk density and apparent bulk density of the CB used in this study were partly obtained from literature and are listed in Table I.

The CB structure is also related to the maximum packing fraction (φ_m), which is defined as the maximum fraction of particles in a given matrix. The DBP value allows one to calculate φ_m in random media according to the following relation:[26]

$$\varphi_m = (1 + \rho DBP)^{-1} \quad (1)$$

where ρ is the density of CB. A value of 1.8 g/mL was used for all types in this study.[26] Equation (1) describes the relationship of φ_m with the morphology of the filler particles. A higher DBP value gives a lower value of φ_m; the data are shown in Table I, which indicate that the critical conductive content of high-structure CB was smaller than that of low-structure CB.[27–30]

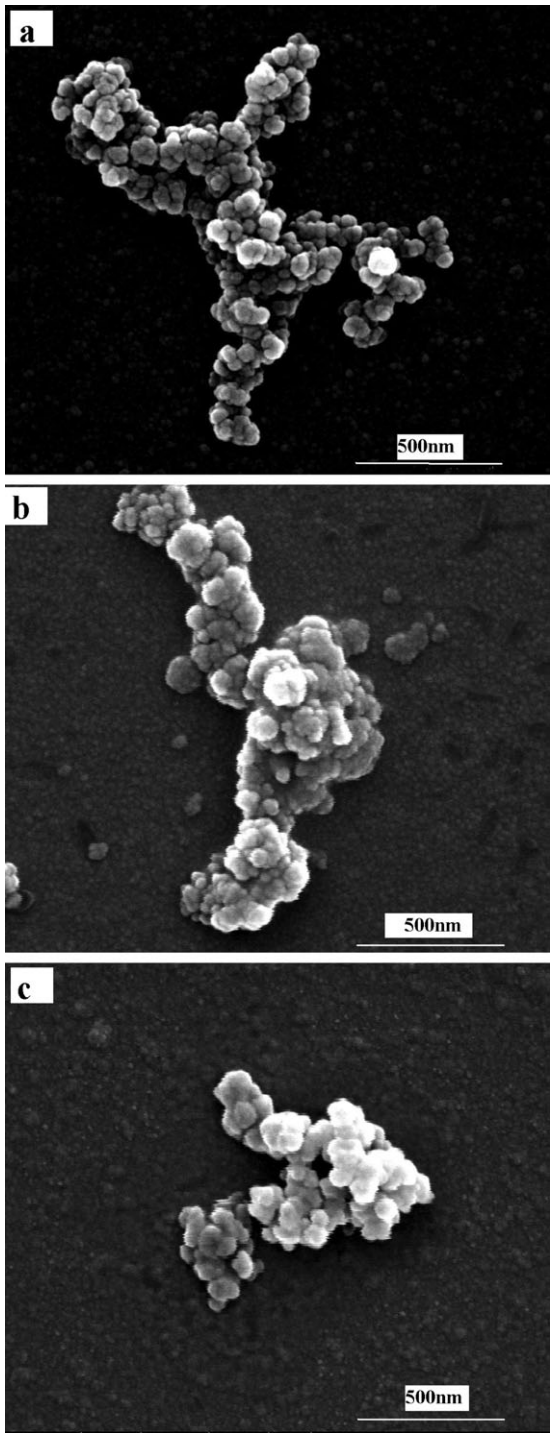

Figure 1. SEM illustration of the CB primary aggregate: (a) 02000, (b) VXC-72, and (c) VXC-68.

Figure 1 is the SEM results of the primary aggregates of the three types of CB used in this study. We can see clearly from Figure 1 that the CB primary aggregates were composed of prime particles. The size and shape of the aggregates and the number of particles per aggregate determined the structure of

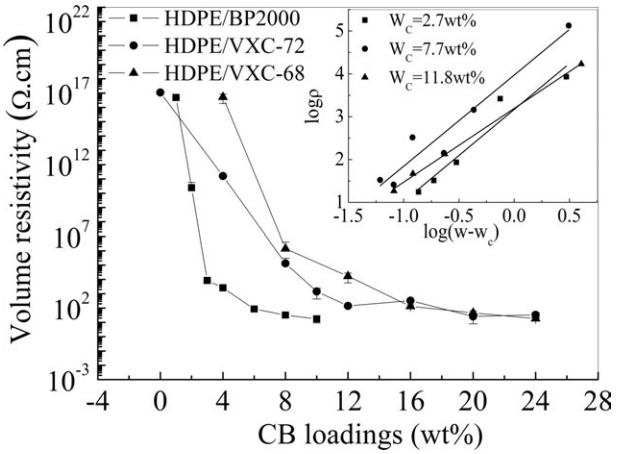

Figure 2. Volume resistivity of the HDPE/CB composites filled with different kinds of CB as a function of the CB loadings. The inserted figure represents the fit to the percolation law.

CB. BP2000 [Figure 1(a)] is a typical highly structured CB, which exhibits a multiarm morphology. The primary aggregate of BP2000 consists of a large number of primary particles that coalesce closely and cannot be destroyed in common processing procedures. However, VXC-72 [Figure 1(b)], which exhibits a relatively linear morphology, indicated a medium structure. VXC-68 [Figure 1(c)], without branching and presenting a spheroidal morphology, exhibited a low structure. Actually, we are the first ones to report the detailed difference in the CB structural morphology by SEM observation among numerous studies.

Electrical Percolation of the HDPE/CB Composites

Figure 2 shows the room-temperature resistivity as a function of the total filler content for the HDPE-based composites with different CB structures. A high level of electrical conductivity was obtained when a connected conductive network was formed at a critical concentration of conductive filler particles. This concentration is usually called the *percolation threshold*.[2–5,17] It can be seen that the room-temperature resistivity of the HDPE/BP2000 composite decreased sharply even at the lower CB content (Figure 2). A power law relation was used to further describe the threshold of the electrical conductivity percolation:

$$\rho \propto (w - w_c)^t \qquad (2)$$

where ρ is the electrical resistivity, w is the mass fraction of CB, w_c is the threshold of the electrical conductivity percolation, and t is the critical exponent. The CB structure affected the threshold behavior of the CPCs, as shown in the inset in Figure 2. The HDPE/BP2000 composite had the smallest percolation threshold ($w_c = 2.7$ wt %), which was far lower than that of the HDPE/VXC-72 ($w_c = 7.7$ wt %) and HDPE/VXC-68 composites ($w_c = 11.8$ wt %). Threshold behavior is one of most remarkable reflections of the ability of particles to build a conductive network in CPCs. Although the HDPE/BP2000 composite had a lower CB content than the HDPE/VXC-68 composite, BP2000 formed a more intensive network. In general, the fact that a composite filled with a high-structure CB has a lower percolation threshold is due to the geometry. CPCs filled with dendritic CB will have a lower percolation threshold than those filled with a spherical one.[31,32]

Temperature-Resistivity Behavior of the HDPE/CB Composites

The temperature-resistivity behavior of CPCs in this study included the PTC/NTC effect and resistance changes during the cooling process. As shown in Figure 3(a), all of the composites (10 wt % BP2000, 20 wt % VXC-72, and 20 wt % VXC-68) provided a similar initial resistivity. This proved that high-structure CB can build a more effective conductive network at lower contents than a low-structure one.

For the HDPE/BP2000 composite, the variation of resistivity was hardly observed during heating; this suggested that the conductive network formed by BP2000 was stable and difficult to destroy. That is, this network was insensitive to temperature. For the HDPE/VXC-72 and HDPE/VXC-68 composites, the resistivity showed a sharp increase for more than one order of magnitude when the temperature reached the T_m of HDPE. In more detail, the PTC effect of the composite was quantified by

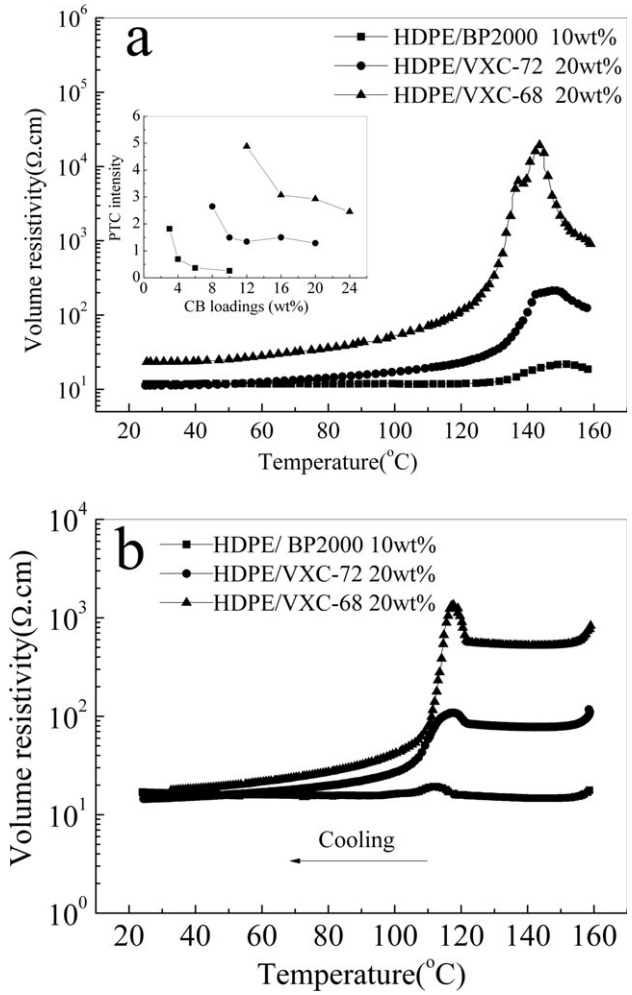

Figure 3. Temperature-resistivity relationship of the HDPE filled with different kinds of CB during the (a) heating and (b) cooling cycles. The inserted figure is the PTC intensity of the CPCs.

Applied Polymer SCIENCE

the PTC intensity, which was obtained from the logarithm value of the ratio of the peak resistivity to the resistivity at room temperature. The PTC intensity was calculated according to the following formula:

$$H_p = \log(\rho_{max}/\rho_{RT}) \quad (3)$$

where H_p is the PTC intensity, ρ_{max} is the maximum resistivity, and ρ_{RT} is the resistivity at room temperature.

The inset of Figure 3(a) shows that the composites containing low-structure CB exhibited a stronger PTC intensity. For the HDPE/BP2000 composite, although the content of CB was 4 wt %, the PTC intensity was less than 1 order of magnitude. For the HDPE/VXC-72 composite containing 8 wt % CB, the PTC intensity was about three orders of magnitude. However, for the HDPE/VXC-68 composite, the PTC intensity was greater than five orders of magnitude when the content of CB was 12 wt %.

The strongest PTC intensity was above the percolation threshold because the conductive network was the most poorly formed at this concentration relative to higher concentrations. With increasing CB content, the PTC intensity of the CPCs became weak. Thermal expansion theory[33–36] is widely applicable for explaining the PTC effect of the CPCs. CB particles were dispersed within the amorphous regions of HDPE instead of within the crystalline regions. When the temperature reached the T_m of HDPE, the melting of the crystalline regions led to a volume expansion of the HDPE matrix, which resulted in the destruction of the conductive network. For the HDPE/BP2000 composite, with more branchy fillers, the effective contact area was larger, so that pulling on them did not separate the particles, such as with spherical particles. Compared to the HDPE/VXC-72 and HDPE/VXC-68 composites, the HDPE/BP2000 composite exhibited a weaker PTC effect. To the contrary, the network built by particles with a spherical morphology was easier to destroy, so the HDPE/VXC-68 composite exhibited a stronger PTC effect. When the temperature increased further, the resistivity of the composites decreased and exhibited the NTC effect; this was related to the reagglomeration of CB particles. As in Figure 3(a), composites filled with low-structure CB showed an obvious NTC effect; meanwhile, the composites containing BP2000 or VXC-72 barely exhibited an NTC effect. The driving force of this effect was the thermal motion of the particles in the melt and the attractive forces between them. The network built by low-structure CB underwent strong deformation in the molten state. The CB clusters were separated and isolated in the melts. With the temperature increase, compared to the branched clusters, the spherical clusters had a stronger ability to move and rebuild a new conductive network.

During the cooling process [Figure 3(b)], the most relevant difference for the three types of composites was the resistivity peaks from 120 to 112°C. We noticed in the composites that the crystallization of the polymer matrix increased the overall resistivity because of the growth of crystal grains interrupted the contacts between the conductive phases. After an increase in the resistivity, with a further decrease in temperature, the HDPE/VXC-68 composite underwent the most drastic conductive decrease. The resistivity diminution was explained by the volume shrinkage; when the samples finished crystallizing, the density of the conductive network increased. At the same time, a significant resistivity decrease in the HDPE/BP2000 composite was hardly observed. The reason why the resistivity of the HDPE/BP2000 composite showed little variation was that the conductive network had a strong built-in matrix and was difficult to change. However, the low-structure CB clusters showed a strong ability to reaggregate and build up connections between the broken network.[10]

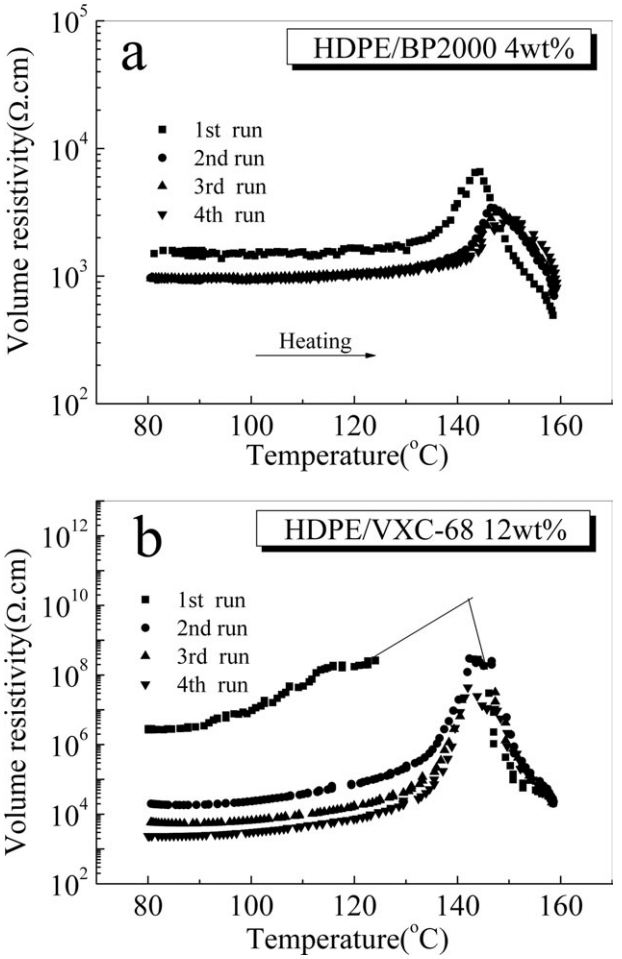

Figure 4. Temperature-resistivity relationship of (a) HDPE/BP2000 (4 wt %) and (b) HDPE/VXC-68 (12 wt %) composites during the heating process.

To further investigate the evolution of conductive network and the reproducibility of the PTC properties of HDPE/CB composites, the samples of HDPE/BP2000 composite containing 4 wt % filler and HDPE/VXC-68 composite containing 12 wt % filler are tested for four heating–cooling cycles. Figure 4 shows resistivity–temperature relationship of the HDPE/BP2000 and HDPE/VXC-68 composites during heating process. The first to third run, the heating rate is 5°C/min and cooling rate is 2°C/min. The fourth run, heating rate is also 5°C/min but cooling rate is 1°C/min to study the effect of cooling rate on the resistivity of composites.

Figure 4a shows the reproducibility of the results of resistivity against temperature for the HDPE/BP2000 composite. Only the

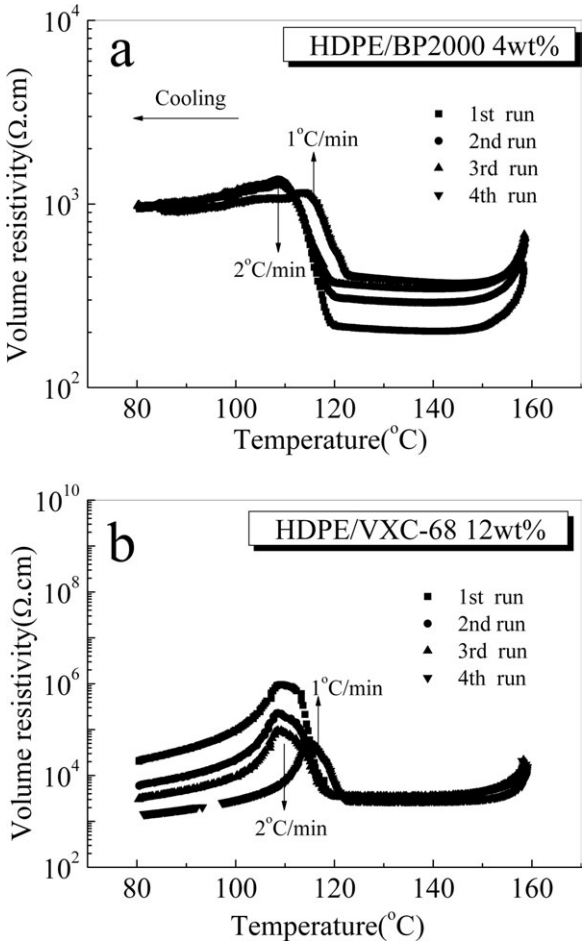

Figure 5. Temperature-resistivity relationship of (a) HDPE/BP2000 (4 wt %) and (b) HDPE/VXC-68 (12 wt %) composites during the cooling process.

first run was different from subsequent ones; this was due to the thermal history during material processing, whereas the later runs had very good reproducibility. However, for the HDPE/VXC-68 composite [Figure 4(b)], the room-temperature resistivity decreased obviously with the heating–cooling cycles. The PTC properties of the HDPE/VXC-68 composite exhibited poor reproducibility compared to those of the HDPE/BP2000 composite. Zhang et al.[9] considered that after compression molding, CPCs have to be regarded as thermodynamic nonequilibrium systems, in which conductive network formation is dependent on the temperature and time. In our system, the conductive network formed by the high-structure CB cluster was more resistant to the heating–cooling cycles than the network formed by the low-structure CB. So the HDPE/BP2000 composite had very good reproducibility. However, for the HDPE/VXC-68 composite, the conductive network formed in compression molding was unstable, and the melting and cooling processes could lead to a more perfect network.[37,38]

Figure 5 shows the resistivity as a function of the temperature in the HDPE/BP200 and HDPE/VXC-68 composites for four heating–cooling cycles during the cooling process. For the HDPE/BP2000 system [Figure 5(a)], the intensity of the resistivity peak from first to third was nearly invariant. However, in the HDPE/VXC-68 system, the resistivity peaks became more insensitive as the cycle times increased. The phenomenon once more showed that a high-structure CB cluster could build a steady, efficient conductive network compared to a low-structure CB cluster. During the heating process, the higher the heating rate was, the higher the starting temperature of the PTC effects was.[39] This was due to the fact that the cutting of the conducting paths of fillers occurred at higher temperature with increasing heating rate. For the purposes of studying the effect of the cooling rate on the starting temperature of the resistivity

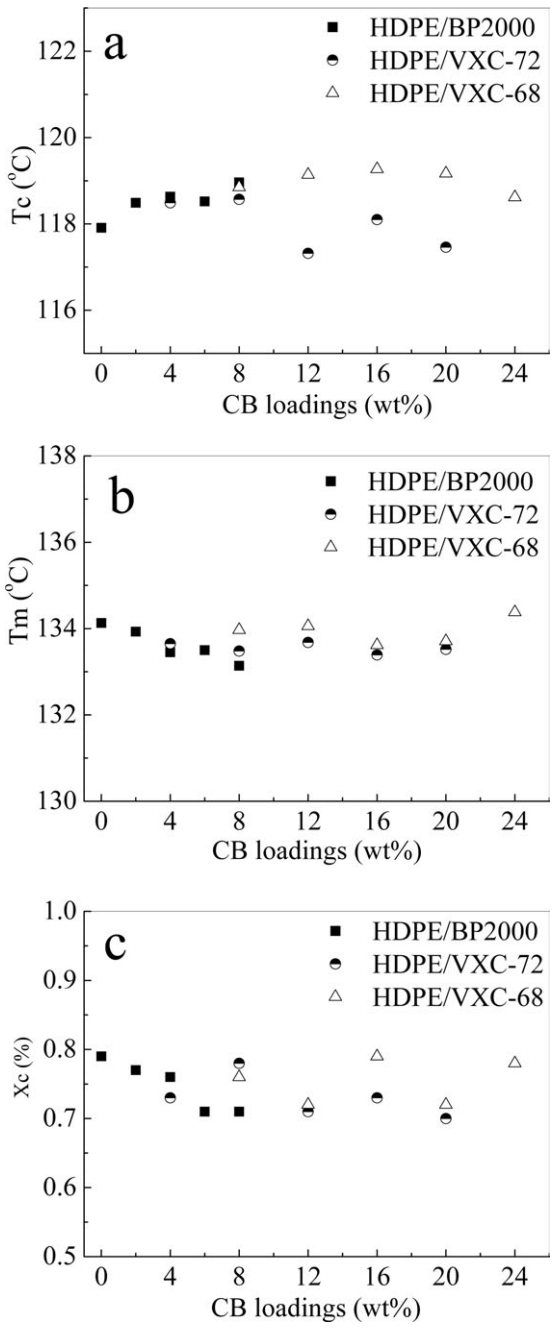

Figure 6. Thermal behavior of the pure HDPE and HDPE/CB composites: (a) T_c, (b) T_m, and (c) X_c.

Applied Polymer SCIENCE

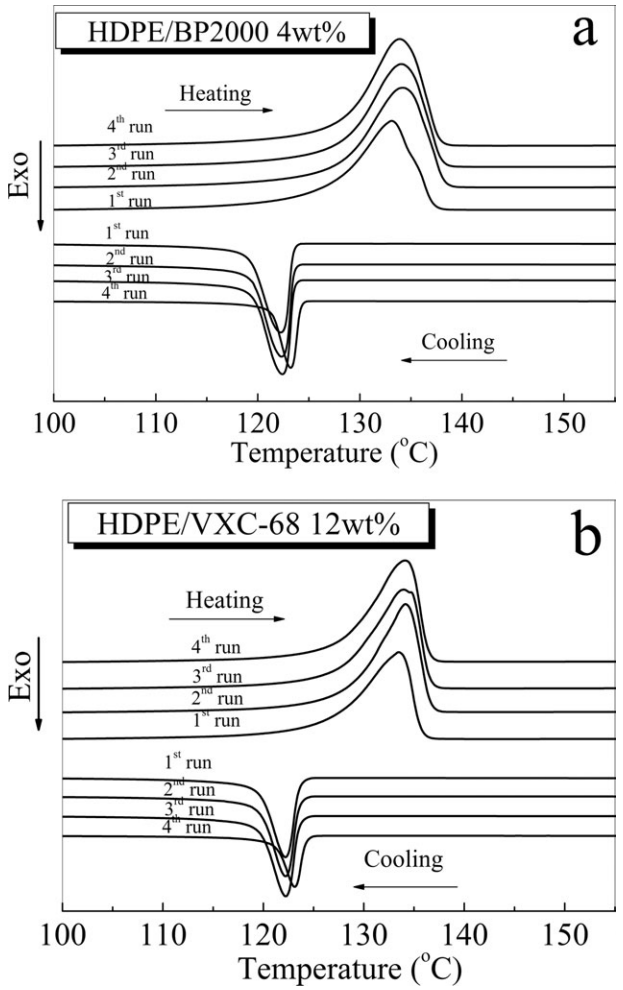

Figure 7. DSC curves of the HDPE/CB composites filled with different kinds of CB: (a) HDPE/BP2000 (4 wt %) and (b) HDPE/VXC-68 (12 wt %) composites.

peak during the cooling process, we reduced the cooling rate (fourth run in Figure 5), and the starting temperature of the resistivity peak moved from 109 to 115°C. This indicated that the lower the cooling rate was, the higher the starting temperature was. We could control the particle network structure by regulating the heating and cooling rates.

Influence of CB on the Crystallization Behavior of the HDPE Matrix

The resistivity peaks appearing during the heating and cooling processes were connected with the melting and crystallization behaviors of the polymer matrix. To clarify this phenomenon, we evaluated the thermal properties of pure HDPE and HDPE/CB composites by DSC. Figure 6 presents the thermal properties of the pure HDPE and HDPE/CB composites. In the figure, T_c is the maximum crystallization temperature, and X_c is the degree of crystallinity, which was calculated by a 100% melting enthalpy of 293 J/g.[1] As shown in Figure 6(a,b), we found that T_c and T_m of pure HDPE remained constant as the CB content and type was varied. Furthermore, compared to the crystallinity of the pure HDPE with HDPE/CB composites [Figure 6(c)], the addition of CB decreased the crystallinity of HDPE (the crystallinity of pure HDPE was 0.79), so the crystallinity was affected by the CB content but was not affected by the CB type.

It is known that the thermal treatment history affects the crystallinity of a semicrystalline polymer. In temperature–resistivity behavior tests, the crystallinity of a polymer affects the PTC effect further.[1] To research the relationship between the reproducibility of the PTC effect and the thermal behavior of polymers, the HDPE/BP2000 composite containing 4 wt % CB and the HDPE/VXC/68 composite containing 12 wt % CB are selected. The samples underwent the same thermal processing as the thermostatic oil bath. Thermograms are shown in Figure 7, and the most detailed thermal data are listed in Table II. After the first heating run, the melting point and crystallinity of the HDPE/BP2000 and HDPE/VXC-68 composites all showed a slight increase. In the later run, the features of the DSC curves were almost the same. In the fourth run, the cooling rate was set to 1°C/min. As shown in Figure 7 and Table II, T_m and crystallinity were not different at various cooling rates, but T_c increased with decreasing cooling rate. Compared to Figure 5, the location of the resistivity peak also moved to higher temperatures for different cooling rates. Therefore, we concluded that the thermal treatment history did not affect the crystallinity of the polymer matrix. The temperature-resistivity behaviors of the composites were influenced by the melting and crystallization of the polymer matrix. T_m and T_c were affected by the heating and cooling rates. We could control the particle network structure by regulating the heating and cooling rates.

CONCLUSIONS

The CB structure was the most important parameter governing the percolation threshold and temperature-resistivity behavior of the CPCs. High-structure CB built an effective conductive network at a low filler content compared to the low-structure one. The reason that a lower percolation threshold formed was geometry; the dendritic particle had a lower percolation than the spherical one. During the heating and cooling processes, the

Table II. DSC Information of the HDPE/BP2000 (4 wt %) and HDPE/VXC-68 (12 wt %) Composites

	HDPE/BP2000			HDPE/VXC-68		
Thermal process	T_c (°C)	T_m (°C)	X_c (%)	T_c (°C)	T_m (°C)	X_c (%)
First run	122.24	133.08	64	122.19	133.45	59
Second run	122.33	134.20	72	122.20	134.10	65
Third run	122.41	134.10	72	122.23	133.99	65
Fourth run	123.30	133.91	72	123.20	134.14	65

resistivity of the CPCs filled with low-structure CB appeared to be a distinct peak; however, for the high-structure CB, the peak was unapparent. That is, composites filled with low-structure CB obtained a stronger PTC intensity than the composites containing the high-structure one. With more dendritic fillers, the effective contact area is larger, so pulling on them does not separate the particles, such as with spherical particles. The reproducibility of the PTC effect of the composites filled with high-structure CB was better than that of the low-structure one. The thermal behavior of HDPE was hardly influenced by the CB content and type but was related to the heating and cooling rates. We could control the location of the resistivity peak by regulating the heating and cooling rates.

ACKNOWLEDGMENT

This research was supported by the National Natural Science Foundation of China (contract grant number 51103087). The authors thank Chen Chen (Center of Analysis and Test of Sichuan University) for the assistance in transmission electron microscopy investigation and Chao Liang Zhang (West China College of Stomatology, Sichuan University) for the SEM observation.

REFERENCES

1. Dai, K.; Li, Z. M.; Xu, X. B. *Polymer* **2008**, *49*, 1037.
2. Huang, J. C. *Adv. Polym. Technol.* **2002**, *21*, 299.
3. Hindermann-Bischoff, M.; Ehrburger-Dolle, F. *Carbon* **2001**, *39*, 375.
4. Balberg, I. *Carbon* **2002**, *40*, 139.
5. Huang, S. L.; Liu, Z. Y.; Yang, M. B. *Macromol. Mater. Eng.* **2012**, *51*, 297.
6. Seo, M. K.; Rhee, K. Y.; Park, S. *J. Curr. Appl. Phys.* **2011**, *11*, 428.
7. Zhang, Y. C.; Huang, Y. F.; Dai, K.; Pang, H.; Chen, C.; Li, Z. M. *Polym.–Plast. Technol.* **2011**, *50*, 1511.
8. Shen, L.; Wang, F.; Yang, H.; Meng, Q. *Polym. Test.* **2011**, *30*, 442.
9. Zhang, C.; Wang, L.; Wang, J.; Ma, C. *Carbon* **2008**, *46*, 2053.
10. Tjong, S.; Liang, G.; Bao, S. *Polym. Eng. Sci.* **2008**, *48*, 177.
11. Jeon, K.; Warnock, S.; Ruiz-Orta, C.; Kismarahardja, A.; Brooks, J.; Alamo, R. G. *J. Polym. Sci. Polym. Phys.* **2010**, *48*, 2084.
12. Deng, H.; Skipa, T.; Zhang, R.; Lellinger, D.; Bilotti, E.; Alig, I.; Peijs, T. *Polymer* **2009**, *50*, 3747.
13. Fernández, M.; Landa, M.; Muñoz, M. E.; Santamara, A. *Eur. Polym. J.* **2011**, *47*, 2078.
14. Alig, I.; Lellinger, D.; Dudkin, S. M.; Pötschke, P. *Polymer* **2007**, *48*, 1020.
15. Lim, G. O.; Min, K. T.; Kim, G. H. *Polym. Eng. Sci.* **2010**, *50*, 290.
16. Li, B.; Zhang, Y. C.; Li, Z. M.; Li, S. N.; Zhang, X. N. *J. Phys. Chem. B* **2010**, *114*, 689.
17. Du, F.; Scogna, R. C.; Zhou, W.; Brand, S.; Fischer, J. E.; Winey, K. *I. Macromolecules* **2004**, *37*, 9048.
18. Pötschke, P.; Abdel-Goad, M.; Pegel, S.; Jehnichen, D.; Mark, J. E.; Zhou, D.; Heinrich, G. *J. Macromol. Sci. Chem.* **2009**, *47*, 12.
19. Park, E. S. *Macromol. Mater. Eng.* **2006**, *291*, 690.
20. Bigg, D. *J. Rheol.* **1984**, *28*, 501.
21. Mallette, J. G.; Quej, L. M.; Marquez, A.; Manero, O. *J. Appl. Polym. Sci.* **2001**, *81*, 562.
22. Probst, N.; Grivei, E. *Carbon* **2002**, *40*, 201.
23. Rahaman, M.; Chaki, T.; Khastgir, D. *J. Mater. Sci.* **2011**, *46*, 3989.
24. Fathi, A.; Hatami, K.; Grady, B. P. *Polym. Eng. Sci.* **2012**, *10*, 1002.
25. Sánchez-González, J.; Macías-García, A.; Alexandre-Franco, M.; Gómez-Serrano, V. *Carbon* **2005**, *43*, 741.
26. Lin, C.; Chung, D. *Carbon* **2007**, *45*, 2922.
27. Zou, J. F.; Yu, Z. Z.; Pan, Y. X.; Fang, X. P.; Ou, Y. C. *J. Polym. Sci. Part B: Polym. Phys.* **2002**, *40*, 954.
28. Pantea, D.; Darmstadt, H.; Kaliaguine, S.; Sümmchen, L.; Roy, C. *Carbon* **2001**, *39*, 1147.
29. Leblanc, J. L. *J. Appl. Polym. Sci.* **2011**, *122*, 599.
30. Morozov, I.; Lauke, B.; Heinrich, G. *Computat. Mater. Sci.* **2010**, *47*, 817.
31. Huang, S. L.; Liu, Z. Y.; Yin, Z. L.; Yang, M. B. *Colloid Polym. Sci.* **2011**, *289*, 1673.
32. Huang, S. L.; Liu, Z. Y.; Yin, Z. L.; Yang, M. B. *Colloid Polym. Sci.* **2011**, *289*, 1927.
33. Ohe, K.; Naito, Y. *Jpn. J. Appl. Phys.* **1971**, *10*, 99.
34. Meyer, J. *Polym. Eng. Sci.* **1973**, *13*, 462.
35. Meyer, J. *Polym. Eng. Sci.* **1974**, *14*, 706.
36. Voet, A. *Rubber Chem. Technol.* **1981**, *54*, 42.
37. Zhang, P.; Xue, W. T.; Zhao, Y.; Liu, P. *J. Appl. Polym. Sci.* **2012**, *123*, 2338.
38. Natsuki, T.; Ni, Q. Q.; Wu, S. H. *Polym. Eng. Sci.* **2008**, *48*, 1345.
39. Xi, Y.; Ishikawa, H.; Bin, Y.; Matsuo, M. *Carbon* **2004**, *42*, 1699.